

OSSOS: IV. DISCOVERY OF A DWARF PLANET CANDIDATE IN THE 9:2 RESONANCE

MICHELE T. BANNISTER¹, MIKE ALEXANDERSEN⁵, SUSAN D. BENECHCHI⁷, YING-TUNG CHEN⁵, AUDREY DELSANTI⁸, WESLEY C. FRASER⁹, BRETT J. GLADMAN¹, MIKAEL GRANVIK¹⁰, WILL M. GRUNDY¹², AURÉLIE GUILBERT-LEPOUTRE³, STEPHEN D. J. GWYN², WING-HUEN IP^{14, 15}, MARIAN JAKUBIK¹⁶, R. LYNNE JONES¹⁷, NATHAN KAIB¹⁸, J. J. KAVELAARS^{1,2}, PEDRO LACERDA⁹, SAMANTHA LAWLER², MATTHEW J. LEHNER^{5, 20, 21}, HSING WEN LIN¹⁴, PATRYK SOFIA LYKAWKA²³, MICHAEL MARSETT^{8, 24}, RUTH MURRAY-CLAY²⁵, KEITH S. NOLL²⁶, ALEX PARKER²⁷, JEAN-MARC PETIT³, ROSEMARY E. PIKE^{1,5}, PHILIPPE ROUSSELOT³, MEGAN E. SCHWAMB³¹, CORY SHANKMAN¹, PETER VERES³⁰, PIERRE VERNAZZA⁸, KATHRYN VOLK⁶, SHIANG-YU WANG⁵, ROBERT WERYK²⁹

¹Department of Physics and Astronomy, University of Victoria, Elliott Building, 3800 Finnerty Rd, Victoria, BC V8P 5C2, Canada

²NRC-Herzberg Astronomy and Astrophysics, National Research Council of Canada, 5071 West Saanich Rd, Victoria, BC V9E 2E7, Canada

³Institut UTINAM UMR6213, CNRS, Univ. Bourgogne Franche-Comté, OSU Theta F25000 Besançon, France

⁴Department of Physics and Astronomy, University of British Columbia, Vancouver, BC, Canada

⁵Institute for Astronomy & Astrophysics, Academia Sinica; 11F AS/NTU, National Taiwan University, 1 Roosevelt Rd., Sec. 4, Taipei 10617, Taiwan

⁶Department of Planetary Sciences/Lunar & Planetary Laboratory, University of Arizona, 1629 E University Blvd, Tucson, AZ 85721, USA

⁷Planetary Science Institute, 1700 East Fort Lowell, Suite 106, Tucson, AZ 85719, USA

⁸Aix Marseille Université, CNRS, LAM (Laboratoire d'Astrophysique de Marseille) UMR 7326, 13388, Marseille, France

⁹Astrophysics Research Centre, Queen's University Belfast, Belfast BT7 1NN, United Kingdom

¹⁰Department of Physics, P.O. Box 64, 00014 University of Helsinki, Finland

¹²Lowell Observatory, Flagstaff, Arizona, USA

¹⁴Institute of Astronomy, National Central University, Taiwan

¹⁵Space Science Institute, Macau University of Science and Technology, Macau

¹⁶Astronomical Institute, Slovak Academy of Science, 05960 Tatranska Lomnica, Slovakia

¹⁷University of Washington, Washington, USA

¹⁸HL Dodge Department of Physics & Astronomy, University of Oklahoma, Norman, OK 73019, USA

²⁰Department of Physics and Astronomy, University of Pennsylvania, 209 S. 33rd St., Philadelphia, PA 19104, USA

²¹Harvard-Smithsonian Center for Astrophysics, 60 Garden St., Cambridge, MA 02138, USA

²³Astronomy Group, School of Interdisciplinary Social and Human Sciences, Kindai University, Japan

²⁴European Southern Observatory (ESO), Alonso de Córdova 3107, 1900 Casilla Vitacura, Santiago, Chile

²⁵Department of Physics, University of California, Santa Barbara, CA 93106, USA

²⁶NASA Goddard Space Flight Center, Code 693, Greenbelt, MD 20771, USA

²⁷Southwest Research Institute, Boulder, Colorado, USA

²⁹Institute for Astronomy, University of Hawaii, 2680 Woodlawn Drive, Honolulu HI 96822, USA

³⁰Jet Propulsion Laboratory, California Institute of Technology, Pasadena, CA 91109, USA

³¹Gemini Observatory, Northern Operations Center, 670 North A'ohoku Place, Hilo, HI 96720, USA

ABSTRACT

We report the discovery and orbit of a new dwarf planet candidate, 2015 RR₂₄₅, by the Outer Solar System Origins Survey (OSSOS). 2015 RR₂₄₅'s orbit is eccentric ($e=0.586$), with a semi-major axis near 82 au, yielding a perihelion distance of 34 au. 2015 RR₂₄₅ has $g - r = 0.59 \pm 0.11$ and absolute magnitude $H_r = 3.6 \pm 0.1$; for an assumed albedo of $p_V = 12\%$ the object has a diameter of ~ 670 km. Based on astrometric measurements from OSSOS and Pan-STARRS1, we find that 2015 RR₂₄₅ is securely trapped in the 9:2 mean-motion resonance with Neptune. It is the first TNO identified in this resonance. On hundred-Myr timescales, particles in 2015 RR₂₄₅-like orbits depart and sometimes return to the resonance, indicating that 2015 RR₂₄₅ likely forms part of the long-lived metastable population of distant TNOs that drift between resonance sticking and actively scattering via gravitational encounters with Neptune. The discovery of a 9:2 TNO stresses the role of resonances in the long-term evolution of objects in the scattering disk, and reinforces the view that distant resonances are heavily populated in the current Solar System. This object further motivates detailed

modelling of the transient sticking population.

Keywords: Kuiper belt objects — individual

1. INTRODUCTION

The Outer Solar System Origins Survey (OSSOS) was designed to provide a set of 500+ very precise trans-Neptunian object (TNO) orbits by the end of its 2013–2017 observations with the Canada-France-Hawaii Telescope (CFHT) (Bannister et al. 2016). As OSSOS covers 155 square degrees of sky on and near the Solar System mid-plane, the Kuiper belt’s steep luminosity function (Gladman et al. 2001; Petit et al. 2011; Fraser et al. 2014) was used to predict that the brightest target expected to be found over the course of the survey would have apparent magnitude $m_r \sim 21.5$. At $m_r = 21.8$, 2015 RR₂₄₅ is the brightest target discovered by OSSOS. At a current heliocentric distance of 65 au, this bright OSSOS detection is also far beyond the median distance of TNO detections in sky surveys. Its substantial distance requires 2015 RR₂₄₅ to be sizeable.

2. DISCOVERY AND SIZE

2015 RR₂₄₅ was discovered with apparent mean magnitude $m_r = 21.76 \pm 0.01$ in three images taken with CFHT MegaCam in an r -band filter over a two-hour span on 9 September 2015 (Table 1). The object is a characterized discovery within the 21 deg² survey region centred at RA 0^h30^m, Declination +5.0°, the seventh of the eight OSSOS survey areas. The discovery analysis was as described in Bannister et al. (2016). A full de-biasing of the region’s discoveries will be accomplished using the OSSOS survey simulator (Bannister et al. 2016) in the future. Because OSSOS reduces an entire discovery semester of data after the semester’s observations are complete, the software first yielded the object in late January 2016. OSSOS imaging is designed to provide tracking throughout the discovery semester; these data quickly yielded further astrometry in September through December 2015.

In February 2016, just before 2015 RR₂₄₅ moved close to solar conjunction, a sequential pair of images in g and r (Table 1) yielded a preliminary broadband colour of $g - r = 0.59 \pm 0.11$. The relatively neutral colour is more common to a dynamically excited “hot” Kuiper Belt object rather than that found in the cold classical belt (Doressoundiram et al. 2005; Peixinho et al. 2015).

We re-observed 2015 RR₂₄₅ in early June 2016 as part of planned OSSOS recovery observations for the fields observed in 2015. 2015 RR₂₄₅ was found to have $m_r \sim 21.8$ (Table 1), consistent with the brightness found in the September 2015 discovery observations. All measurements can be retrieved from the IAU Minor Planet Center (MPC)¹; photometry referred to here is summarized in Table 1.

Based on the heliocentric distance (see § 3), the absolute magnitude H_r is 3.6 ± 0.1 ($H_V = 3.8 \pm 0.1$ ²). The albedos for $2 < H_V < 4$ TNOs that have been determined by thermal measurements range between $p_V = 7\%$ (2002 MS₄; $H_V = 4.0$) and 21% (Quaoar; $H_V = 2.7$) (Brucker et al. 2009). For an assumed albedo p_V at each end of this range, duller or more reflective respectively, 2015 RR₂₄₅’s diameter is 870–500 km. For an albedo of 9% like that of $H_V = 2.0$ TNO 2007 OR₁₀ (Andras et al. 2016), which is on a comparable orbit ($a=67$ au, $q=33$ au) at a current distance of 88 au (Schwamb et al. 2010), 2015 RR₂₄₅’s diameter would be 770 km. The neutral colour of 2015 RR₂₄₅ leans it towards being part of the neutral colour class, which has lower albedos of $\sim 6\%$ (Lacerda et al. 2014). However, due to the wide range of albedos seen for objects in this H_V range (Lellouch et al. 2013), we adopt a modal albedo of $p_V = 12\%$ ($D \sim 670$ km) in the rest of this discussion.

The plausible diameter range for 2015 RR₂₄₅ is interesting because it spans the range of sizes where significant changes occur in TNO surface composition, particularly with the presence of deep water ice absorption (Brown 2012). At this size scale, objects with the expected ice/rock compositional mix predominant in the outer Solar System are expected to adjust to an approximately spherical hydrostatic equilibrium shape (Tancredi & Favre 2008; Lineweaver & Norman 2010). The majority of the possible diameter range places 2015 RR₂₄₅ in the size range where spherical alteration occurs. By this criterion it could be considered one of the roughly 20–30 “dwarf planet candidates” now known from previous wide-field shallow surveys covering most of the sky (Larsen et al. 2007; Trujillo & Brown 2003; Schwamb et al. 2010; Sheppard et al. 2011; Rabinowitz et al. 2012; Bannister 2013; Brown et al. 2015), most of which have $a < 50$ au. There are likely another few dozen similarly large objects in very large- a orbits; when far from perihelion they would be sufficiently faint to only be found with wide-field optical searches on > 4 m telescopes.

michele.t.bannister@gmail.com

¹ http://www.minorplanetcenter.net/db_search/show_object?utf8=%E2%9C%93&object_id=2015+RR245

² $H_V = H_r - 0.03 + 0.45(g - r)$ (Smith et al. 2002)

Table 1. Selected observations with CFHT MegaCam of 2015 RR₂₄₅

Time (UT)	Filter	Exposure Time (s)	Magnitude	IQ (")	Target Elongation (°)
2015 09 09.37654	R.MP9602	300	21.77 ± 0.02	0.42	159.3
2015 09 09.42092	R.MP9602	300	21.77 ± 0.02	0.42	159.3
2015 09 09.46188	R.MP9602	300	21.73 ± 0.02	0.42	159.4
2016 02 04.22299	R.MP9602	200	22.04 ± 0.06	1.21	51.4
2016 02 04.22679	G.MP9402	200	22.63 ± 0.07	1.56	51.4
2016 06 07.61302	R.MP9602	300	21.94 ± 0.03	0.55	69.5
2016 06 08.57085	R.MP9602	300	21.88 ± 0.02	0.60	70.4

NOTE—The photometry is calibrated to the SDSS per the methodology in [Bannister et al. \(2016\)](#). The filter bandpasses are similar to those of Sloan.

3. ORBIT

With all available OSSOS astrometry from September 2015 to June 2016, the distance to 2015 RR₂₄₅ could be accurately evaluated as 64.479 ± 0.008 au. However, the barycentric orbital semi-major axis was less precisely determinable: $a = 82.1 \pm 2.5$ AU (1-sigma covariance-based error estimate). With a swath of semi-major axis uncertainty more than five au wide, it was impossible to confidently determine resonance occupation: typical resonance widths are 0.5–1 au in the outer Solar System. Without a very precise orbit, multiple dynamical behaviours are possible, and this object could not usefully advance the discussion of the subtleties of resonance sticking below. At this point the object was released to the MPC so that the worldwide community could participate in the second year of recovery and provide physical characterization. On July 13, 2016, the Pan-STARRS1 survey ([Kaiser et al. 2010](#)) released six oppositions of astrometry of 2015 RR₂₄₅ to the MPC, spanning Sept 2010 to July 2015. A subset of these observations were found independently by the analysis of [Weryk et al. \(2016\)](#); they were augmented with additional Pan-STARRS1 detections found based on the [Weryk et al. \(2016\)](#) orbit.

The orbital solution to the seven-opposition set of astrometric measurements (calculated per [Bernstein & Khushalani 2000](#)) provides a secure classification when analyzed with the dynamical orbital classification algorithm of [Gladman et al. \(2008\)](#): all plausible orbits yield the same dynamical behaviour. The best-fit J2000 barycentric orbital elements are given in Table 2. Fig. 1 shows the large span of all plausible orbital elements obtained by the Metropolis algorithm described by [Gladman et al. \(2008\)](#). The span of plausible orbital behaviours gives a secure dynamical classification in the 9:2 mean-motion resonance with Neptune (Fig. 2), which is centred³ at a barycentric semi-major axis of 81.96 au. 2015 RR₂₄₅ is the first trans-Neptunian object securely identified in this distant resonance.

Table 2. Barycentric elements for 2015 RR₂₄₅ in ICRS at osculating epoch 2457274.9

a (au)	e	i (°)	Ω (°)	ω (°)	JD peri
81.86 ± 0.05	0.5859 ± 0.0003	7.553 ± 0.001	211.761 ± 0.002	260.817 ± 0.012	2485409 ± 10

NOTE—Barycentric distance: 64.479 ± 0.001 au with true anomaly $f = 253.5^\circ$.

Ω is the longitude of ascending node, ω the argument of perihelion, and $JD\ peri$ is the Julian day of osculating barycentric perihelion. The uncertainties are the 1σ estimates based on the covariance matrix at the best-fit orbit, derived by the method of [Bernstein & Khushalani \(2000\)](#).

³ Note that this evaluation should be made in barycentric orbital element space. Neptune’s barycentric semi-major axis $a_N = 30.07$ au is perturbed by up to 0.02 au on 500-Myr time scales. For instance, while the barycentric mean centre of the resonance is shifting on the 10 Myr interval in Fig. 2 (upper row), it is not apparent due to being $\sim 1/200^{th}$ the barycentric oscillation of the particles.

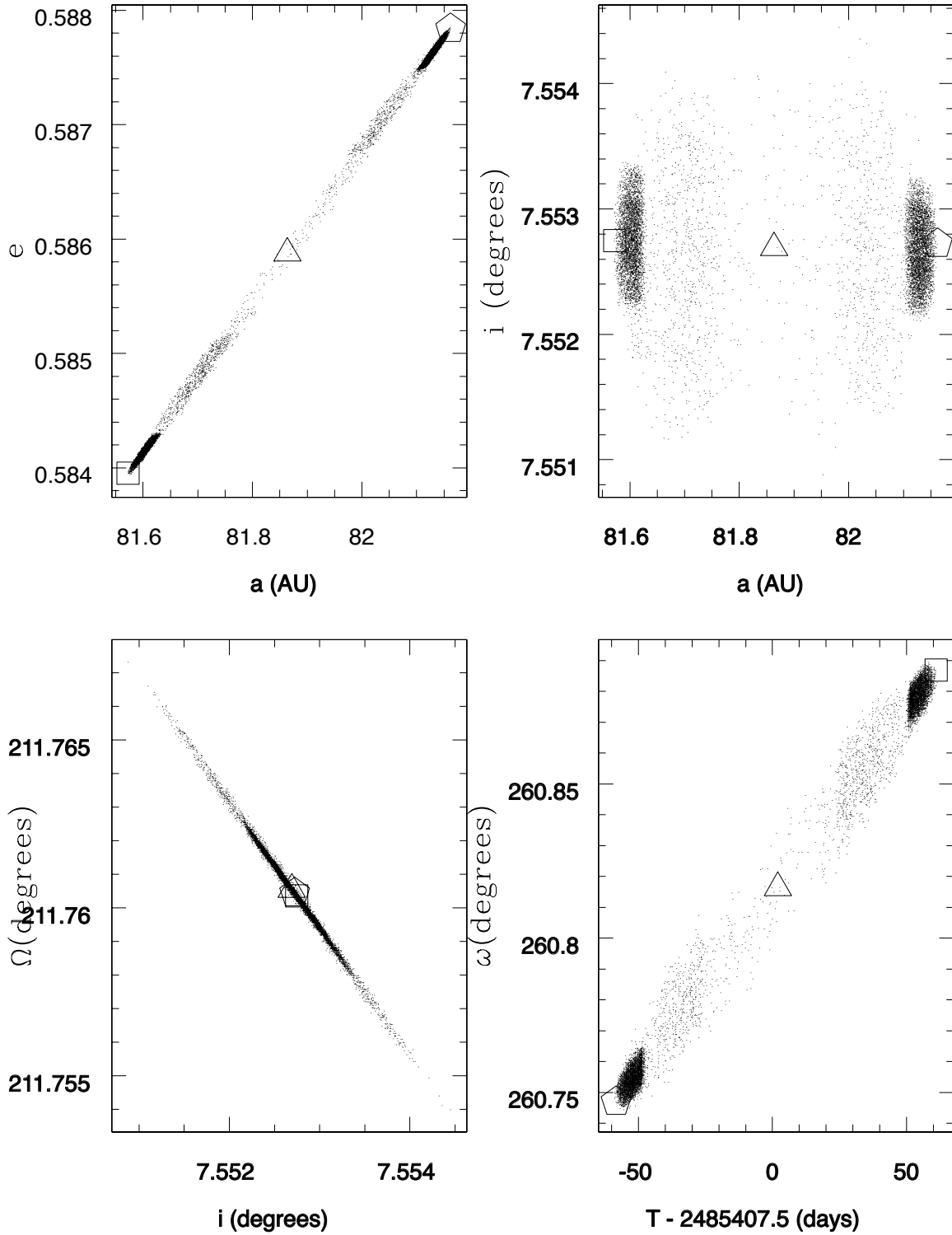


Figure 1. Uncertainties on the orbit of 2015 RR₂₄₅ using the accounting for possible systematics fully described in Gladman et al. (2008). The best-fit orbit (Table 2) is marked by the large open triangle in each panel, while the square and pentagon give orbital elements corresponding to the minimal and maximal semi-major axes (respectively) of the Monte Carlo search. Small dots show orbits consistent with the available astrometry found during the search for the two extremal orbits; their density is not proportional to likelihood and are not used elsewhere in this manuscript. All elements are barycentric in the J2000 reference frame and thus judged relative to the ecliptic. (upper left) Semi-major axis a versus eccentricity e . Note the strong correlation that is equivalent to a set of orbits having nearly the same $q=33.9$ au perihelion distance as the best fit orbit. (upper right) Ecliptic inclination i as a function of a . (lower left) Longitude of ascending node Ω as a function of i . (lower right) Argument of perihelion ω versus the Julian day of osculating perihelion judged at the epoch JD= 2457274.9.

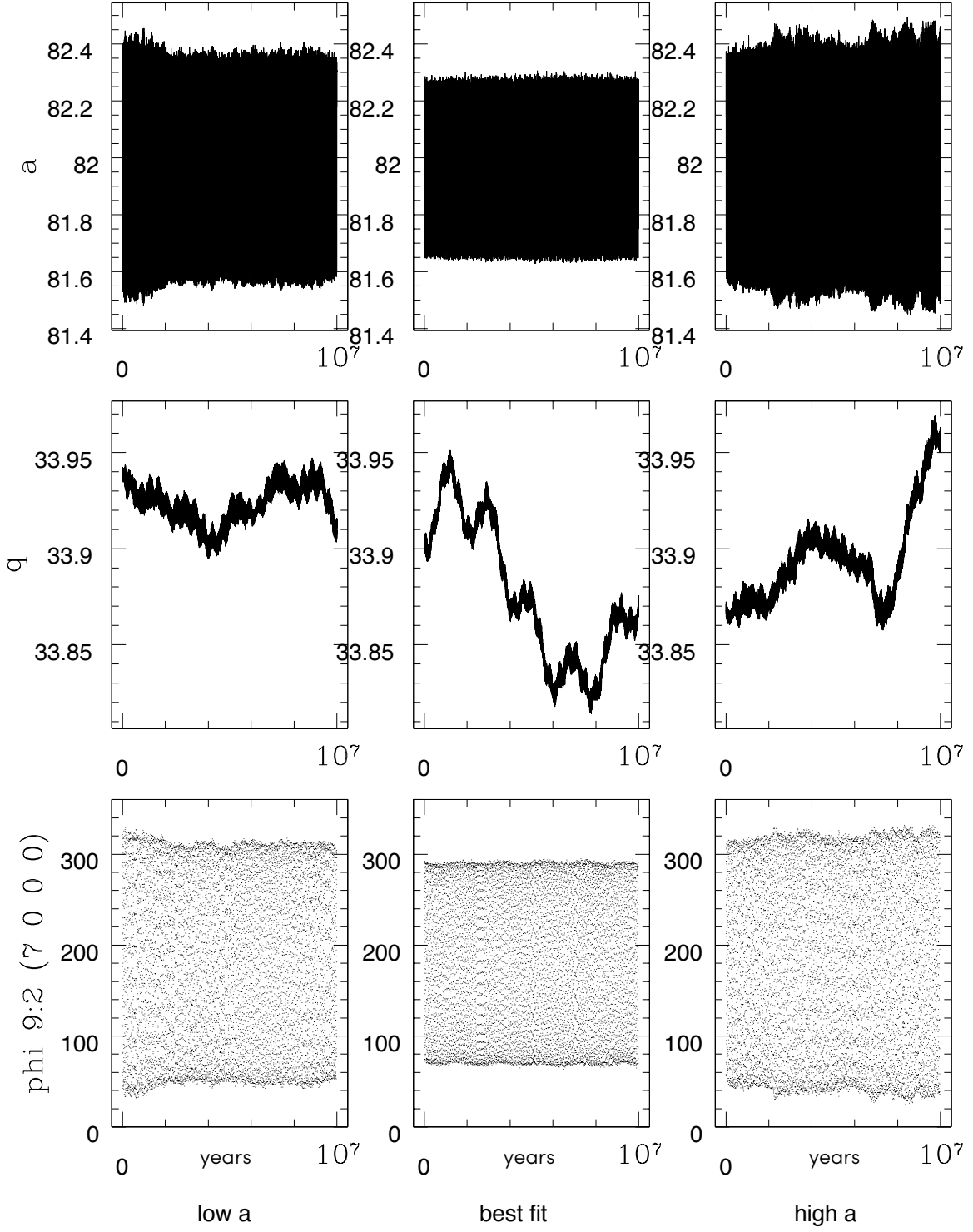


Figure 2. The orbital evolution of the three orbits marked in Fig. 1. The left, middle, and right columns show the a , q , and resonant argument Φ evolution for the minimal, best-fit, and maximal semi-major axis orbits. The $\simeq 0.5$ au oscillation of a is forced by the resonance and is coupled to the rapid ($\simeq 10,000$ year) libration of the resonant argument. The dynamical protection provided by the resonance results in only very weak interactions allowing only very slow evolution of the perihelion distance q . The libration amplitude in the resonance is $\simeq 110^\circ$ for the best fit orbit and is 20–30 degrees larger for the extremal orbits.

This resonance occupancy reinforces the finding that there are many TNOs in high-order, distant $a > 50$ resonances (Chiang et al. 2003; Lykawka & Mukai 2007a; Gladman et al. 2008; Gladman et al. 2012; Alexandersen et al. 2014; Pike et al. 2015; Sheppard et al. 2016; Kaib & Sheppard 2016). Objects in large- a resonances are inefficiently discovered due to the r^{-4} dependence for reflected flux, the overall steep TNO luminosity function, and because the large eccentricities

of such orbits places most of the population at large distances at any given time, and thus below the flux limit of wide-field surveys. When carefully debiased for detectability, the large- a resonances together yield a total resonant population that is comparable to the main classical Kuiper belt (Gladman et al. 2012; Pike et al. 2015; Volk et al. 2016).

The resonant protection provided by the 9:2 resonance is very similar to that provided by the 3:2 and 5:2 mean-motion resonances (Cohen & Hubbard 1965; Gladman et al. 2012). Specifically, libration of the resonant argument $\Phi_{92} = 9\lambda - 2\lambda_N - 7\varpi$ around 180° (Fig. 2) means that when a resonant TNO is at perihelion, Neptune is never near the same mean orbital longitude λ_N , preventing close encounters (in this expression, λ is the mean longitude of the particle and $\varpi = \Omega + \omega$ is the longitude of perihelion). The libration amplitude L_{92} results in the perihelion longitude offset between the TNO and Neptune varying from $90^\circ - L_{92}/2$ to $90^\circ + L_{92}/2$. Using methods described in Volk et al. (2016), the L_{92} distribution (Fig. 3) was determined with 10 Myr simulations of 250 particles (‘clones’) distributed probabilistically in the 3σ error ellipse card on the covariance matrix based on the orbit best-fit. All these orbits remained resonant for the 10 Myr duration; at the current epoch, 2015 RR₂₄₅ is thus firmly lodged in the resonance.

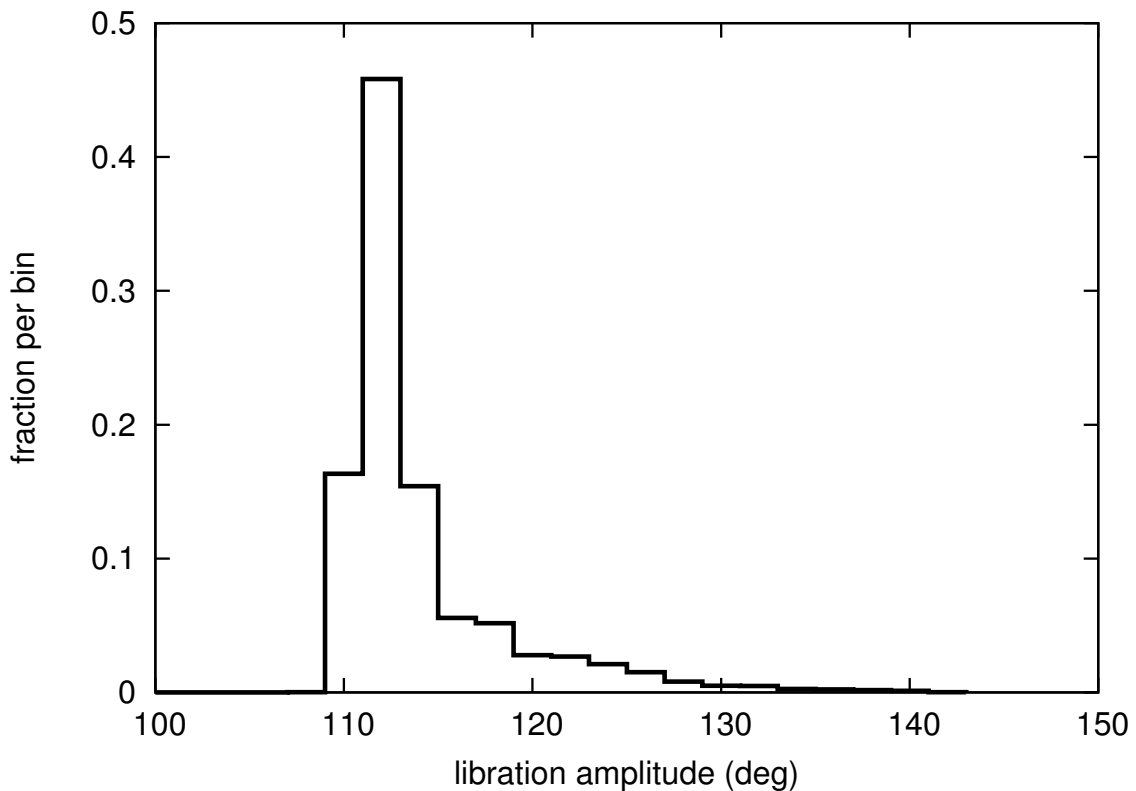


Figure 3. Histogram of the L_{92} libration amplitude distribution of the 250 clones produced by the covariance matrix analysis. See text for discussion.

There are many resonant TNOs with precisely known orbits that are stable for the lifetime of the Solar System, Pluto being an obvious example. There also exist TNOs with similar high-precision orbits whose orbital evolution shows many resonant librations for all clones initially, but then have nearly all clones leave the resonance on time scales $\ll 4$ Gyr. Several Neptune 1:1 resonators (Trojans) are known to exhibit this phenomenon (Horner & Lykawka 2012; Alexandersen et al. 2014), as do three well-studied TNOs in the 5:1 (Pike et al. 2015). It is thus important to keep in mind the distinction between (1) actively ‘scattering’ TNOs, (2) ‘temporarily’ metastable TNOs, (3) stable resonators and (4) permanently detached TNOs with no chance of recoupling on solar-system time scales; orbital resonances are often involved when TNOs transit between those states.

To explore the longer-term evolution of 2015 RR₂₄₅, we extended the integration of these same 250 clones to 500 Myr. While every orbit initially spends at least 10 Myr steadily librating in the resonance, the clones begin to diffuse out on time scales of 50 Myr and begin actively scattering due to Neptune (Fig. 4). Their subsequent evolution then becomes diffusive, with the scattering particles sometimes temporarily sticking to other resonances (during which the

evolution shows a stable semi-major axis at some other value). Particles commonly return to stick to the 9:2 resonance itself, and then remain stuck for typical time scales of tens of Myr. We find a median dynamical lifetime before first departure from the resonance of order 100 Myr, with roughly 15% of the clones in the resonance 500 Myr in the future (note that some may have left and returned; Fig. 4). Only a tiny fraction of the clones will be in the 9:2 after 4 Gyr. It is thus very likely that 2015 RR₂₄₅ has not continuously spent the last 4 Gyr in the resonance, but instead was trapped from the actively scattering population within the last ~ 100 Myr.

4. DISCUSSION

Two main possibilities appear likely for how 2015 RR₂₄₅ came to be in its current orbit: first, that it was scattered off Neptune and is presently ‘sticking’ to a resonance, with the scattering event either recent or early in Solar System history. Secondly, 2015 RR₂₄₅ could have been captured into the resonance during Neptune’s migration. We consider each in turn.

Metastable resonant TNOs that are emplaced by ‘transient sticking’ are an established phenomenon. The transient sticking slows orbital evolution, providing a mechanism necessary to maintain the current scattering disk, which would otherwise decay on timescales much shorter than the age of the Solar System (Duncan & Levison 1997). Several studies of transient sticking report temporary captures in the 9:2 resonance (Fernández et al. 2004; Lykawka & Mukai 2007b; Almeida et al. 2009). These studies found most periods spent in the resonance are short (~ 10 Myr) and with large libration amplitudes $L_{92} > 130^\circ$. However, occasionally their modelled particles attained smaller libration amplitudes, which lengthened their occupation in the resonance. The low-libration ‘sticker’ objects provide an enhanced contribution to the steady-state transient population. Indeed, the simulations reported in Lykawka & Mukai (2007b) include stickers in the 9:2 resonance with L_{92} as small as the $\simeq 115^\circ$ observed for 2015 RR₂₄₅. Of the particles in Lykawka & Mukai (2007b) surviving to the present time, roughly half had experienced a trapping in the 9:2 at some time, and one case kept $L_{92} < 120^\circ$ for 700 Myr (P. Lykawka, 2016 private communication). 2015 RR₂₄₅ plausibly fits into this ‘metastable TNO’ paradigm.

Given the ~ 100 Myr median resonant lifetime of our orbital clones, we suggest that 2015 RR₂₄₅ is likely to be transiently alternating between Neptune mean-motion resonances and the actively scattering component of the trans-Neptunian region. This conclusion is bolstered by 2015 RR₂₄₅’s perihelion distance of $q = 34$ au; roughly⁴ $q < 37$ au results in the continuing orbital interactions with Neptune that are shared by almost all active scatterers. In fact, non-resonant TNOs with q only 4 au from Neptune’s orbital semi-major axis of 30 au typically experience sufficiently numerous strong encounters with Neptune (when the longitude of Neptune matches that of the TNO while the TNO is at perihelion) for their orbits to rapidly evolve (Morbidelli et al. 2004). Such rapidly evolving orbits, when observed at the current epoch, are classified in the scattering population (Gladman et al. 2008). Residence in the 9:2 or other resonances can temporarily shield TNOs from scattering, but eventually their orbital evolution will lead such TNOs to leave the resonance and resume active scattering. Note that there can be resonant objects (eg. Pluto) which do not participate at all in this process on 4 Gyr time scales.

Though we consider transient sticking the most plausible origin for 2015 RR₂₄₅, other emplacement scenarios are possible. For example, Nice model-type histories (Levison et al. 2008) could in principle emplace objects in the 9:2 resonance directly during an early Solar System upheaval event. If fortunate enough to remain stable for the subsequent ~ 4 Gyr solar system age, these objects might still be present today. A numerical simulation of TNO sculpting under a Nice model-like Solar System history (Pike et al. 2016) does produce a population of 9:2 resonant TNOs. However, the objects reported in Pike et al. (2016), drawn from the simulations of Brasser & Morbidelli (2013) may also be transient captures. Further work is needed to determine whether these objects were caught early and retained, or whether they are in fact transiently sticking TNOs captured later in the 4 Gyr numerical evolution.

Alternately, resonance capture during smooth migration of Neptune, even over a relatively large 10 au distance, would require an initial disk extending beyond 55 au to provide a source of TNOs for capture into resonance. While there are low-inclination TNOs beyond the 2:1 resonance that suggest that the cold classical TNO population did extend to at least 50 au (Bannister et al. 2016), 55 au would be at the larger end of the observed debris disk population (Hillenbrand et al. 2008). Because they appeal to capture early in the Solar System’s history, both the Nice-type and the smooth migration scenarios would require that future observations of 2015 RR₂₄₅ push its orbit to a subset of phase space more stable than that currently explored by our orbital clones; this seems unlikely given the extent of our numerical exploration.

⁴ Orbital integration is required; see discussions in Lykawka & Mukai (2007a) and Gladman et al. (2008).

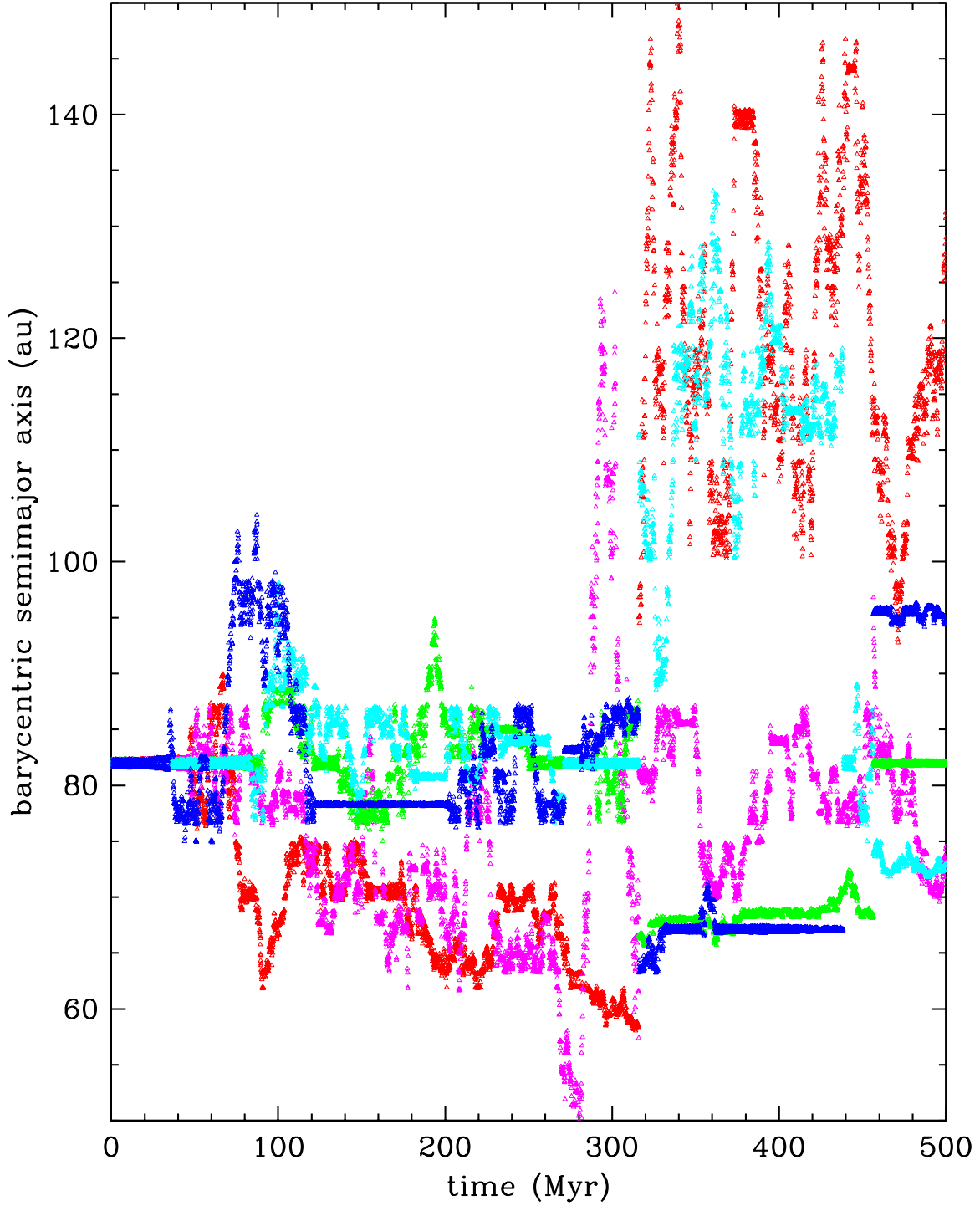


Figure 4. Semi-major axis evolution for 5 sample orbits (each a different colour) drawn from a covariance-based set of 250 orbits consistent with the astrometry of 2015 RR₂₄₅. For the first 40 Myr, all 250 clones oscillate by the $\simeq 1$ au full width of the resonance. They then begin leaving the resonance into the actively scattering population where their semi-major axes are changing by several au/Myr in a diffusive manner driven by Neptune scattering. The median time before first departure from the resonance is $\simeq 100$ Myr; here 5 orbits with less typical early departures are shown, sometimes displaying the frequently seen behaviour among the clone ensemble of subsequent sticking to other resonances or return to the 9:2.

We next consider whether our detection of a large TNO in the resonant phase of the metastable population is consistent with the population ratios between the two phases (scattering/resonant). Our initial numerical experiments suggest that—summed over all resonances—the transiently stuck population may be comparable to the population of active scatterers. This is similar to the behaviour seen for the known 5:1 resonant TNOs, which typically spend half their lifetimes in various resonances and half in a scattering state (Pike et al. 2015). If so, a single transiently-stuck dwarf planet candidate detection by OSSOS is consistent with our lack of detection of similarly-sized active scatterers. Only a few of the well-populated distant resonances are known to contain $H < 4$ TNOs (Sheppard et al. 2011). Additionally, the classification methods of Elliot et al. (2005) and Gladman et al. (2008) both agree that with its current astrometric measurements, 2007 OR₁₀ is securely in the 10:3 resonance. Because dynamical timescales are longer at large semi-major axes, transiently stuck TNOs spend more time in more distant (low-order) resonances, making the 9:2 a reasonable resonance in which to find 2015 RR₂₄₅.

When viewed in absolute magnitude H space, detection of an $H_r = 3.6$ TNO by OSSOS is naively a $\sim 4\%$ probability using the TNO sky density estimates of Fraser et al. (2014, figure 9). However, the H_r frequency distribution reported in Fraser et al. (2014) utilizes an empirical formulation that adjusts for the increased albedos of many large TNOs (Brown 2008; Fraser et al. 2008, 2014). Use of that relation⁵ to compute an ‘effective’ H_r for 2015 RR₂₄₅ results in a value of $H_{r,eff} = 4.35$. At this $H_{r,eff}$, our detection of one TNO in 155 square degrees of survey coverage is in good agreement with the measured $H_{r,eff}$ frequency distribution.

Concentrating on such ‘large’ TNOs, 2015 RR₂₄₅ spends approximately two-thirds of its orbit brighter than the shallowest magnitude limit $m_r \sim 24.5$ of any OSSOS block; even at aphelion its sky motion of $\sim 1''$ /hour would be easily detectable by our survey. With such a substantial visibility fraction, a trivial estimate of the number of comparable TNOs within about 10 degrees of the ecliptic is $(360 \times 20/155) \simeq 50$ $H_r < 3.6$ TNOs over the sky, with only a small upward correction (of $<50\%$) for the fraction of the visibility. Demanding that these TNOs be also in the 9:2 should be viewed as dangerous ‘post-facto’ reasoning (in that the argument would apply to any sub-population in which the single TNO was found). Instead, the perspective should be that there are 50-100 $H_r < 3.6$ TNOs in the volume inside 100 au, which seems completely plausible. Its dynamics suggest 2015 RR₂₄₅ is one of the objects that survived the population decay in the initially scattered disk after experiencing scattering and temporary capture in multiple resonances. If of order 100 $H \lesssim 4$ TNOs exist and the “retention efficiency” over the entire outer Solar System is $\sim 1\%$ (Duncan & Levison 1997; Nesvorný & Vokrouhlický 2016), then there would have been $\sim 10,000$ such objects present in the outer Solar System at the time that the giant planets began to clear the region. This is in line with primordial estimates (Stern 1991; Stern & Colwell 1997) of ~ 1000 Plutos, when one takes into account that Pluto-scale TNOs are only a fraction of the $H < 4$ inventory.

Viewed another way, there may still be an issue due to the puzzling fact that 2015 RR₂₄₅ is roughly 3 magnitudes brighter than the OSSOS detection limits. That is, OSSOS detects many TNOs with $m_r < 24.8$, and none are in the 9:2 resonance⁶. If one anchors a normal exponential magnitude distribution to 2015 RR₂₄₅, even restricting to its discovery distance of 65 AU, there should be ~ 100 TNOs up to three magnitudes fainter, yet none have been found. The problem is worsened when considering that near the $q = 34$ au perihelion distance, TNOs as faint as $H_r \simeq 9$ are visible to OSSOS, and detection of those TNOs is far more likely than finding 2015 RR₂₄₅. A plausible resolution of this apparent paradox is most likely that 2015 RR₂₄₅ has an albedo that is higher than that of smaller TNOs (Stansberry et al. 2008), as suggested above, and thus this TNO does not anchor a steep exponential distribution. Considering known large TNOs on potentially ‘metastable’ orbits, for an albedo like that of the substantially larger Eris (at a current heliocentric distance of 96 au) of $p \simeq 0.96$ (Sicardy et al. 2011), the effective H_r becomes nearly 6, and the non-detection of smaller TNOs even at perihelion is not statistically alarming. We point out, however, that the 1500 km diameter 2007 OR₁₀’s visual albedo is only 9% (Andras et al. 2016), raising doubt on whether all large TNOs have high albedos (Brown 2008). Future thermal measurements and spectral studies of 2015 RR₂₄₅, which will steadily brighten as it approaches its 2090 perihelion, will inform the open question of its albedo and surface composition.

This research was supported by funding from the National Research Council of Canada and the National Science and Engineering Research Council of Canada. The authors recognize and acknowledge the sacred nature of Maunakea, and appreciate the opportunity to observe from the mountain. This project could not have been a success without the dedicated staff of the Canada–France–Hawaii Telescope (CFHT) telescope. Based on observations obtained with

⁵ The H_r mag of the 2015 RR₂₄₅ is used to estimate a size given an estimated intrinsic albedo of $p_V = 12\%$ and then an ‘effective’ H_r mag is computed for that size using an effective albedo of 6%.

⁶ No other published surveys suggest a small TNO being detected in the 9:2 either.

MegaPrime/MegaCam, a joint project of CFHT and CEA/DAPNIA. CFHT is operated by the National Research Council of Canada, the Institut National des Sciences de l’Univers of the Centre National de la Recherche Scientifique of France, and the University of Hawaii, with OSSOS receiving additional access due to contributions from the Institute of Astronomy and Astrophysics, Academia Sinica, Taiwan. This work is based in part on data produced and hosted at the Canadian Astronomy Data Centre. MES was supported by the Gemini Observatory, which is operated by the Association of Universities for Research in Astronomy, Inc., on behalf of the international Gemini partnership of Argentina, Brazil, Canada, Chile, and the United States of America.

Facilities: CFHT (MegaPrime), Pan-STARRS1

Software: Python, astropy, matplotlib, scipy, numpy, supermongo, SWIFT

REFERENCES

- Alexandersen, M., Gladman, B., Kavelaars, J. J., et al. 2014, arXiv.org, 1411.7953v1
- Almeida, A. J. C., Peixinho, N., & Correia, A. C. M. 2009, *Astronomy and Astrophysics*, 508, 1021
- Andras, P., Kiss, C., Müller, T. G., et al. 2016, arXiv.org, arXiv:1603.03090
- Bannister, M. T. 2013, PhD thesis, RSAA, the Australian National University., Canberra
- Bannister, M. T., Kavelaars, J. J., Petit, J.-M., et al. 2016, in press, *Astronomical Journal*, arXiv:1511.02895
- Bernstein, G., & Khushalani, B. 2000, *The Astronomical Journal*, 120, 3323
- Brasser, R., & Morbidelli, A. 2013, *Icarus*, 225, 40
- Brown, M. E. 2008, in *The Solar System Beyond Neptune* (The University of Arizona Press), 335–344
- . 2012, *Annual Review of Earth and Planetary Sciences*, 40, 467
- Brown, M. E., Bannister, M. T., Schmidt, B. P., et al. 2015, *The Astronomical Journal*, 149, 1
- Brucker, M. J., Grundy, W. M., Stansberry, J. A., et al. 2009, *Icarus*, 201, 284
- Chiang, E. I., Jordan, A. B., Millis, R. L., et al. 2003, *Astronomical Journal*, 430
- Cohen, C. J., & Hubbard, E. C. 1965, *Astronomical Journal*, 70, 10
- Doressoundiram, A., Peixinho, N., Doucet, C., et al. 2005, *Icarus*, 174, 90
- Duncan, M. J., & Levison, H. F. 1997, *Science*, 276, 1670
- Elliot, J. L., Kern, S. D., Clancy, K. B., et al. 2005, *The Astronomical Journal*, 129, 1117
- Fernández, J. A., Gallardo, T., & Brunini, A. 2004, *Icarus*, 172, 372
- Fraser, W. C., Brown, M. E., Morbidelli, A., Parker, A., & Batygin, K. 2014, *The Astrophysical Journal*, 782, 100
- Fraser, W. C., Kavelaars, J. J., Holman, M. J., et al. 2008, *Icarus*, 195, 827
- Gladman, B., Kavelaars, J. J., Petit, J.-M., et al. 2001, *The Astronomical Journal*, 122, 1051
- Gladman, B., Marsden, B. G., & Vanlaerhoven, C. 2008, in *The Solar System Beyond Neptune*, ed. M. A. Barucci, H. Boehnhardt, D. P. Cruikshank, A. Morbidelli, & R. Dotson (The University of Arizona Press), 43–57
- Gladman, B., Lawler, S. M., Petit, J.-M., et al. 2012, *The Astronomical Journal*, 144, 23
- Hillenbrand, L. A., Carpenter, J. M., Kim, J. S., et al. 2008, *ApJ*, 677, 630
- Horner, J., & Lykawka, P. S. 2012, *Monthly Notices of the Royal Astronomical Society*, 426, 159
- Kaib, N. A., & Sheppard, S. S. 2016, arXiv.org, 1607.01777v1
- Kaiser, N., Burgett, W., Chambers, K., et al. 2010, in *SPIE Astronomical Telescopes + Instrumentation*, ed. L. M. Stepp, R. Gilmozzi, & H. J. Hall (SPIE), 77330E–14
- Lacerda, P., Fornasier, S., Lellouch, E., et al. 2014, arXiv.org, 1406.1420v1
- Larsen, J. A., Roe, E. S., Albert, C. E., et al. 2007, *The Astronomical Journal*, 133, 1247
- Lellouch, E., Santos-Sanz, P., Lacerda, P., et al. 2013, *Astronomy and Astrophysics*, 557, A60
- Levison, H. F., Morbidelli, A., Vanlaerhoven, C., Gomes, R., & Tsiganis, K. 2008, *ICARUS*, 196, 258
- Lineweaver, C. H., & Norman, M. 2010, eprint arXiv:1004.1091, astro-ph.EP
- Lykawka, P. S., & Mukai, T. 2007a, *Icarus*, 186, 331
- . 2007b, *Icarus*, 192, 238
- Morbidelli, A., Emel’yanenko, V. V., & Levison, H. F. 2004, *Monthly Notices of the Royal Astronomical Society*, 355, 935
- Nesvorný, D., & Vokrouhlický, D. 2016, *The Astrophysical Journal*, 825, 1
- Peixinho, N., Delsanti, A., & Doressoundiram, A. 2015, *Astronomy and Astrophysics*, 577, A35
- Petit, J.-M., Kavelaars, J. J., Gladman, B. J., et al. 2011, *The Astronomical Journal*, 142, 131
- Pike, R. E., Kavelaars, J. J., Petit, J.-M., et al. 2015, *The Astronomical Journal*, 149, 1
- Pike, R. E., Lawler, S., Brasser, R., et al. 2016, submitted to *AJ*
- Rabinowitz, D., Schwamb, M. E., Hadjijska, E., & Tourtellotte, S. 2012, *The Astronomical Journal*, 144, 140
- Schwamb, M. E., Brown, M. E., Rabinowitz, D. L., & Ragozzine, D. 2010, *The Astrophysical Journal*, 720, 1691
- Sheppard, S. S., Trujillo, C., & Tholen, D. J. 2016, arXiv.org, 1606.02294v1
- Sheppard, S. S., Udalski, A., Trujillo, C., et al. 2011, *The Astronomical Journal*, 142, 98
- Sicardy, B., Ortiz, J. L., Assafin, M., et al. 2011, *Nature*, 478, 493
- Smith, J. A., Tucker, D. L., Kent, S., et al. 2002, *The Astronomical Journal*, 123, 2121
- Stansberry, J., Grundy, W., Brown, M. E., et al. 2008, in *The Solar System Beyond Neptune* (The University of Arizona Press), 161–179
- Stern, S. A. 1991, *Icarus* (ISSN 0019-1035), 90, 271
- Stern, S. A., & Colwell, J. E. 1997, *The Astronomical Journal*, 114, 841
- Tancredi, G., & Favre, S. 2008, *Icarus*, 195, 851
- Trujillo, C. A., & Brown, M. E. 2003, *Earth*, 92, 99
- Volk, K., Murray-Clay, R., Gladman, B., et al. 2016, *Astronomical Journal*, 152, 23
- Weryk, R. J., Lilly, E., Chastel, S., et al. 2016, submitted to *Icarus*, arXiv:1607.04895